



# Nonlinear increase of Greenland Ice Sheet runoff into Disko Bay

Steffen Hetzinger<sup>1</sup>, Jochen Halfar<sup>2</sup>, Takaaki K. Watanabe<sup>1,3</sup>, Alexandra Tsay<sup>4</sup>

<sup>1</sup>Institute of Geosciences, Kiel University, Kiel, 24118, Germany

<sup>5</sup>5 Laboratory Chemical Physical Sciences Department, University of Toronto Mississauga, Mississauga, ON, L5L 1C6, Canada

<sup>3</sup>KIKAI Institute for Coral Reef Sciences, Kikai Town, Kagoshima, 891-6151, Japan

<sup>4</sup>Department of Earth Sciences, University of Geneva, Geneva, CH-1205, Switzerland

*Correspondence to:* Steffen Hetzinger (steffen.hetzinger@ifg.uni-kiel.de)

**Abstract.** The Greenland Ice Sheet (GrIS) has experienced accelerated mass loss with record peaks in 2012 and 2019. Despite its role as an important tipping element in the climate system, the GrIS's response to recent warming is poorly understood. Here we use Ba/Ca ratios in coralline algae as a proxy for runoff into Disko Bay which is strongly influenced by the input of meltwater from glaciers connected to the GrIS, particularly from Jakobshavn Glacier - the fastest flowing marine-terminating glacier of the GrIS. The 115-year multispecimen master chronology confirms an unprecedented trend change in runoff beginning in the early 2000s. Statistical trend- and time of emergence analysis of the algal proxy record suggests that in 2007 western GrIS runoff has permanently emerged above the 20th century reference period, while temperature observations have not yet exceeded this threshold. This provides independent evidence for a non-linear accelerated response of the largest GrIS glacier, underscoring modelling results that a tipping point in glacial mass balance might soon be reached. Massive GrIS meltwater influx could intensify upper ocean stratification and contribute to global sea level rise.

## 20 Short summary

The Greenland Ice Sheet is a climate tipping element; most glaciers have retreated and Arctic warming has accelerated, yet Greenland Ice Sheet response and mass-loss estimates remain uncertain and likely underestimated. Using Ba/Ca ratios from a >100-year coralline algal record, we reconstruct seasonal runoff variability into Disko Bay surface waters and find a nonlinear rise in western Greenland Ice Sheet runoff since the early 2000s, now permanently exceeding variability of the 20th century.

25

## 1 Introduction

In 2023, summer surface air temperatures were the warmest ever observed in the Arctic, while the highest point on the Greenland ice sheet (GrIS) experienced melting for only the fifth time in a 34-year observation record (Ballinger et al., 2023). Estimates of GrIS annual melt anomalies indicate that the mass loss has been accelerating since the mid-1990s due to increased ice discharge into the ocean, melting and runoff. This change in state has been attributed to rising atmospheric and ocean temperatures (Hanna et al., 2021) and a decrease in surface albedo leading to enhanced melt-albedo feedbacks (Hofer et al., 2017). Warming over the GrIS now exceeds the range of pre-industrial temperature variability in the past millennium based on ice core reconstructions (Hörhold et al., 2023). Many of the GrIS's glaciers are currently undergoing accelerated ablation,



thus providing increasing inflows of meteoric water to the ocean (Bamber et al., 2012, 2018; Velicogna, 2009). The GrIS mass loss is well reflected in marine-terminating glaciers in western Greenland, which have increased their discharge rates over the last decades (King et al., 2018, 2020; Mankoff et al., 2019). Prior to 2009, it was estimated that about 50 to 60% of GrIS loss was from acceleration of outlet glaciers (Rignot et al., 2010). However, since 2009, the relative importance of runoff as a cause of ice sheet mass loss has increased, and now accounts for >60% of the increase (King et al., 2020). In the 2012 record-year 35 GrIS surface melting was more expansive than at any time over the period of available satellite measurements, followed by record melting in 2019, driven by a summer heatwave (Tedesco and Fettweis, 2020) in the Arctic. Between 1992 and 2020 40 melting of the polar ice sheets has caused a 21 mm rise in global sea level, with ice loss from Greenland accounting for almost two-thirds (13.5 mm) of this rise (Otosaka et al., 2023). Recent rapid mass loss of the GrIS has led to large increases in 45 freshwater fluxes from Greenland into the North Atlantic and is changing the freshwater budget of the Arctic and sub-polar North Atlantic Oceans (Bamber et al., 2012, 2018). The western side of the Greenland ice sheet has been identified as the primary area of mass loss (Mouginot et al., 2019; Nick et al., 2013). Surface ocean waters in Disko Bay, the site of this study 50 (Fig. 1), are strongly influenced by the input of meltwater from glaciers connected to the GrIS, particularly from Jakobshavn Glacier (Jakobshavn Isbræ, JI; Sermeq Kujalleq), the fastest flowing marine-terminating glacier of the GrIS (Joughin et al., 2020). Hydrographic studies describe a seasonal freshening of the surface ocean due to JI glacial discharge (Hansen et al., 2012; Hopwood et al., 2025; Latuta et al., 2025) across large areas of Disko Bay, including our study sites (Mascarenhas and Zielinski, 2019) (Figure 1). Remarkably, around half of the entire GrIS mass loss between 2000 and 2012 can be attributed to just four glaciers, while over the entire observation period (1972-2018), JI stands out as the largest contributor to mass loss 55 (Mouginot et al., 2019). The drainage area of JI covers a substantial part of central-West-Greenland (about 6.5% (Echelmeyer et al., 1991) of the area of the GrIS). Recent satellite data (Greene et al., 2024; Sasgen et al., 2020) reveal new acceleration in mass loss, with record losses observed in 2012, 2019 and 2022.

Ocean temperature changes in Disko Bay have likely had a long-term controlling influence on JI, but the linkage between 60 ocean circulation and atmospheric influence in West Greenland surface waters is complex (Holland et al., 2008). Significant changes in oceanographic conditions in Disko Bay have taken place since the mid-1990s, when an increased inflow of warmer Atlantic waters led to a transition from a cold to a warm regime (Hansen et al., 2012; Holland et al., 2008). Warming of subsurface waters was most prominent at 200-250 m water depth, leading to a temperature increase of several °C in the early 65 2000s (Hansen et al., 2012; Joughin et al., 2012, 2020; Khazendar et al., 2019). This warming had a significant effect on JI leading to disintegration of the floating ice tongue in the late 1990s and early 2000s, when the glacier began to speed up (Joughin et al., 2004). The speed-up peaked in the summer of 2012 and similar large speed-ups occurred over the next several summers (Joughin et al., 2020), when warmer subsurface waters entered the ca. 40 km long Ilulissat Icfjord.

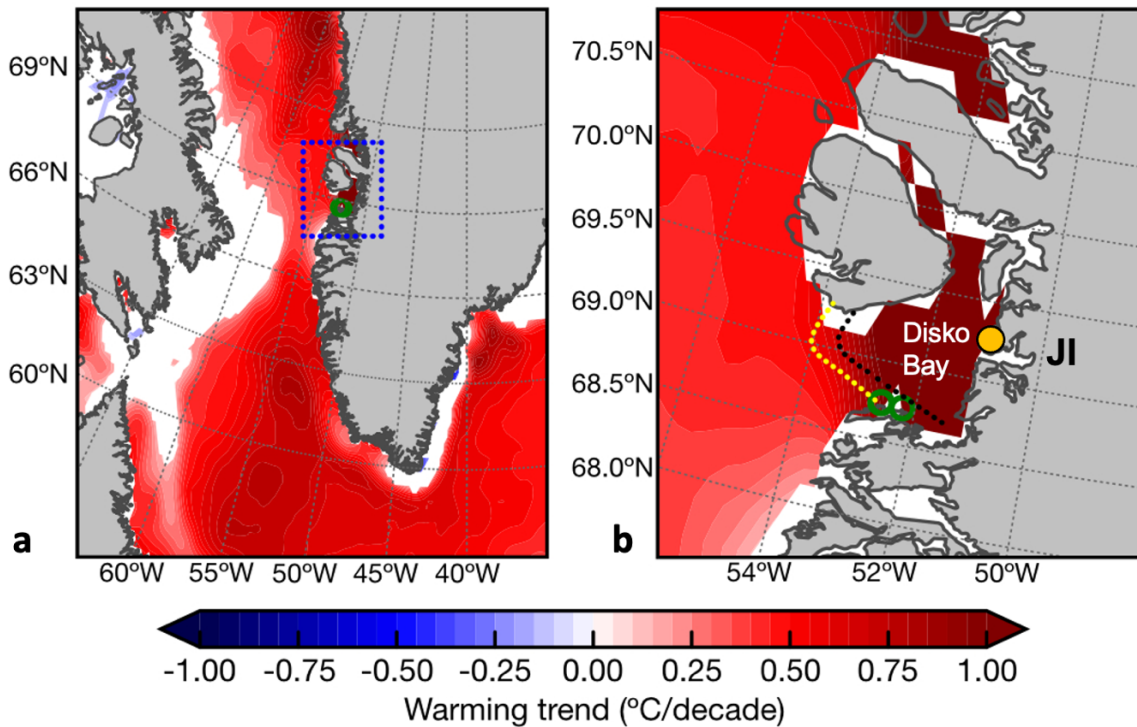


**Figure 1. West Greenland surface water temperature warming trend.** a) Temperature trends ( $^{\circ}\text{C}/\text{decade}$ ) for the period 1982-2020 for summer sea surface temperature (SST, JJA, OISSTv2p1;  $0.25 \times 0.25^{\circ}$  resolution, 1982-2020) for oceanic regions offshore of (a) southern and (b) central-western Greenland. b) Disko Bay region in central-western Greenland (rectangle, enlarged in a) with locations of sampling sites (green circles) southwest of Jakobshavn Glacier (Jakobshavn Isbrae, JI). Trend calculation significant at 90%. Locations of Ilulissat (orange circle, weather station 4221) and Jakobshavn Isbrae are indicated. Outline of Disko Bay frontal zone surface water mass (based on salinity from hydrographic observations in summer 2017 (Mascarenhas and Zielinski, 2019)) is marked as yellow stippled line ( $< 33$  psu) to indicate up to where glacial freshwater influences surface water in relation to our study sites. Glacial meltwater plume extent marked as black stippled line.

70

75

However, due to a lack of long-term multidecadal-length continuous oceanographic measurements in Disko Bay, effects of increased GrIS melting on the surface ocean are not well understood and widely undocumented. Satellite observations indicate that warming of sea surface temperatures (SSTs) in Disko Bay (central-western Greenland) is exceptional and much faster than in other regions, reaching a warming of  $>1^{\circ}\text{C}/\text{decade}$  since 1982 (Figure 1). Tracing glacial meltwater in Greenland's boundary currents and into the deep-water-formation regions is a major challenge requiring enormous observational and modelling efforts (Martin and Biastoch, 2023).

80  
85  
Although the GrIS's marine-terminating glaciers transport and subsequently deposit vast quantities of sediment into the ocean, there are no long-term datasets monitoring sediment transport from the marine margins, either by iceberg-rafting, or from subglacial plumes (Andresen et al., 2024). In total, the GrIS contributes 8% to the global ocean sediment budget (Overeem et al., 2017). Concentrations of trace elements in subglacial meltwaters of GrIS glaciers are generally high, mainly derived from the biogeochemical weathering of underlying bedrock, hence subglacial runoff is exporting globally significant amounts of



trace elements into the oceans (Hawkins et al., 2020). Areas with pronounced glacial meltwater input often exhibit sediment plumes with localized enrichments of a range of trace elements (Krause et al., 2021), including barium (Guo et al., 2025). Previous research has demonstrated that barium, when transported in fine-grained suspended sediments, can undergo 90 desorption in the surface ocean layer, subsequently behaving as a conservative tracer in Arctic waters (Guay and Kenison Falkner, 1998).

Available reconstructions of glacial discharge rely mostly on short periods of satellite observations and model data (Karlsson et al., 2023), or historical photographs (Khan et al., 2020), which are insufficient to describe potential long term changes occurring in shallow marine ecosystems. Limited temporal resolution and often discontinuous measurement time series cannot 95 provide records of adequate length needed for assessing interannual- to decadal-scale variability and trends. Thus, long-term continuous proxy reconstructions from the surface ocean can provide additional understanding of glacier–ocean interactions, and for modeling past and future ice sheet changes (Joughin et al., 2012). Long-lived coralline algae (genus *Clathromorphum* sp.) have been used to develop century-scale annually-resolved continuous reconstructions of past environmental and climate variability in high-latitude oceans (Halfar et al., 2013; Hetzinger et al., 2019). Slow growth rates (<50-500µm/year) and clear 100 annual banding (similar to tree rings) permit the development of sub-annually resolved reconstructions from the surface ocean layer.

Seasonally resolved coralline algal Ba/Ca ratios have previously served to reconstruct changes in past glacier-derived meltwater input in high-Arctic Svalbard (Hetzinger et al., 2021), successfully tracking changes in regional glacier mass balance and runoff. Ba/Ca ratios are a proxy for reconstructing past variability in the input of terrestrial material, runoff and sediment 105 flux in a number of environments using organisms that produce calcium carbonate skeletons (Chan et al., 2011; Evans et al., 2015; Gillikin et al., 2006; Grove et al., 2013; Kniest et al., 2024; McCulloch et al., 2003; Weldeab et al., 2007). Ba/Ca ratios in biogenic carbonate directly reflect seawater Ba/Ca variability in culture experiments (Yamazaki et al., 2021). Here, we present a multi-specimen master chronology of coralline algal Ba/Ca ratios from Disko Bay, Greenland, to show that recent 110 rates of runoff are unprecedented in the past 115 years, signalling the permanent emergence of western GrIS mass change above the 20th century threshold. This is highly significant as the proxy is suggesting that the increase in glacial runoff is faster than expected from surface temperature evolution alone.

## 2 Methods

### 2.1 Sample collection

115 In summer 2016 several *C. compactum* coralline algae were discovered and collected in Disko Bay, Greenland (Fig. 1). In June 2019, a more systematic exploration for long-lived *C. compactum* algae was undertaken resulting in a large collection of high-quality coralline algal samples (*C. compactum*, more than 150 samples) in southern Disko Bay. Sampling took place near site 16-1 (2016), at site 19-9 (2019, within 1 km of site 16-1) and site 19-10 (2019, ca. 15 km eastwards towards Jakobshavn Glacier, Fig. 1). At the study sites, live coralline algal buildups were removed from rocky substrate using chisel and hammer 120 via SCUBA at 10 m water depth. Algal specimens suitable for sclerochronological and geochemical analysis were chosen



according to size (taller specimens = longer record) and smoothness of sample surface (smoother surface = better developed internal growth increments and lower degree of bioerosion – based on previous experience).

## 2.2 Sample preparation

125 Coralline algal specimens were cut vertically to a thickness of ~1 cm using a rock saw. Afterwards, thick sections (2 mm) were cut from the slabs. Before microscopic scanning, thick section surfaces were polished using diamond-polishing suspensions (grit sizes of 9, 3, and 1  $\mu\text{m}$ ) using a polishing disk (Struers Labopol). An Olympus reflected light microscope (VS-BX) with an automated sampling stage and imaging system, using the geo.TS (Olympus Soft Imaging Systems), was employed to generate high-resolution images of the polished sample surfaces. With this setup, all sample surfaces were mapped  
130 two-dimensionally at different magnifications. Using the resultant high-resolution photomosaics, algal growth increment patterns can be mapped laterally, also allowing the inspection of sample quality, and identification of areas which are potentially not usable for following laser ablation analysis (see Figure A1). For each sample thick section two reference points and multiple potential paths for laser line transects were marked on the high-resolution photomosaics using geo.TS software. Line transects were placed perpendicular to the direction of algal growth. This digitized information, including laser line  
135 transect positions, was then copied to the LA-ICP-MS system, where the sample was recoordinated, overlaying the live sample image with the transferred paths. Subsequently, the final laser line transects could be positioned precisely over the digitized paths based on the high-resolution photomosaics.

## 2.3 Geochemical sample analysis by LA-ICP-MS

140 Geochemical analyses of nine samples were performed in the Laser Ablation-Inductively Coupled Plasma Mass Spectrometry (LA-ICP-MS) laboratory at the University of Geneva, Switzerland.  $^{43}\text{Ca}$ ,  $^{24}\text{Mg}$ , and  $^{137}\text{Ba}$  contents were measured with a NWR-193 HE laser ablation unit connected to an Agilent 8900 triple-quadrupole ICP-MS. Prior to measurement, each specimen was pre-ablated to eliminate potential surface contaminants, and transects were positioned to avoid conceptacles. Analyses were carried out with laser energy densities of  $6 \text{ J/cm}^2$ , laser pulse rate of 10 Hz and helium as carrier gas. The rectangular laser slot  
145 size was  $70 \times 10 \mu\text{m}$ , with the long axis aligned parallel to algal growth increments. Individual line transects up to  $6000 \mu\text{m}$  length were ablated at a scan rate of  $5 \mu\text{m/sec}$ . The ICP-MS was configured to acquire ~6.5 measurements per second, yielding a sampling resolution of  $0.775 \mu\text{m}$ . Multiple parallel transects (some overlapping) were measured on each sample to assess sample heterogeneity and to verify reproducibility. Calcium concentrations obtained by ICP-OES (Hetzinger et al., 2011) served as the basis for using  $^{43}\text{Ca}$  as the internal standard. To correct for potential instrumental drift, NIST SRM 610 glass (US  
150 National Institute of Standard and Technology Standard Reference Material) was analyzed twice per hour for 60 sec as an external standard. Drift remained negligible throughout the analyses, with standard deviations consistently below 10%. Additional methodological details for LA-ICP-MS analysis on *C. compactum*, including external reproducibility for elemental ratios (e.g. Mg/Ca, Ba/Ca) and detection limits, are provided in (Hetzinger et al., 2011). Data reduction was carried out using a customized in-house spreadsheet designed for line-transect inputs.



155

## 2.4 Development of Chronologies

Chronologies were constructed by identifying and counting the annual growth increments on the digitized photomosaics of each specimen. Because all material was collected alive, the outermost (top) layer was assigned the collection year. Distinct annual growth layers are marked by bands of short, densely calcified cells that develop in late autumn and winter during the 160 formation of reproductive sporangia (conceptacles) (Adey et al., 2013; Halfar et al., 2013). Although the growth banding is typically well-defined, banding can occasionally be obscured by invertebrate grazing, boring, or other forms of surface disturbance. Elevated Mg concentrations within the *Clathromorphum* skeleton are interpreted as indicators of summer growth. Age models were created by combining the distinct seasonal cycle in algal Mg/Ca ratios with the visually identified annual 165 growth increment banding. For Disko Bay samples, peak maximum Mg/Ca values were aligned with August - the warmest month on average - while minimum values were assigned to March, the coldest month. The Mg/Ca records were then linearly interpolated between these seasonal anchor/tie points using AnalySeries (Paillard et al., 1996), producing an evenly spaced proxy time series with 12 data points per year. To refine the chronologies and to identify potential agemodel inconsistencies, annual Mg/Ca extrema were compared with the mapped growth band structure for each individual algal growth year. Mean 170 annual extension rates for Disko Bay specimens were calculated from the widths of Mg/Ca cycles, yielding an average of 201  $\mu\text{m}/\text{year}$  ( $n=9$ , range 164-244  $\mu\text{m}$ ). The longest continuous record is preserved in sample 16-1-19 (1903-2015).

In total, nine coralline algal specimens were analyzed using the LA-ICP-MS technique, extending from 1897-2019. Geochemical laser data are available from 1903 onwards (Figure 2, Figure A2). Annually averaged Ba/Ca ratio time series 175 were calculated from monthly-resolved time series. Annual mean values of geochemical data are calculated until 2018 (seven samples collected in summer 2019) and until 2015 (two samples collected in summer 2016), respectively. This constitutes a common time period of 52 years (1963-2015) where all samples overlap, while individual samples extend much longer until the beginning of the 20th century, i.e. representing a 115 year continuous annually averaged record (Figure 2). The multi-specimen intersample average record/master chronology was calculated by averaging all data for overlapping time periods 180 (1932 to 2018:  $n=5$  from 1932;  $n=7$  from 1950;  $n=9$  from 1963 to 2018; see Figure A2). The confidence interval of the master chronology record was derived from the bootstrap technique with 20,000 loop iterations.

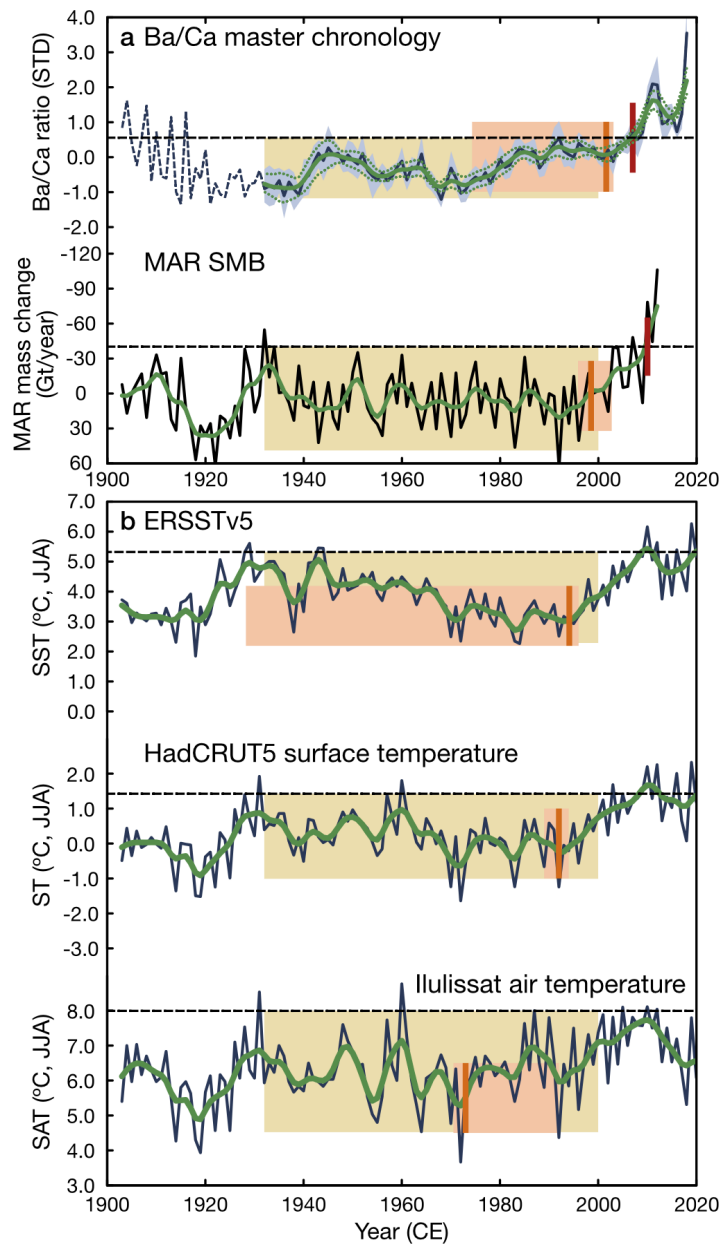


**Figure 2. Algal proxy, model-based GrIS surface mass balance and temperature. a)** Normalized and annually averaged algal Ba/Ca master chronology (average of nine individual algal records) in comparison to modelled surface mass balance (SMB) for western Greenland (MAR3.5.2; note that mass change data is plotted inversely, Gigaton per year (Gt/year)). Correlations significant at 99% level (15pt Gaussian filtered records,  $R = -0.54$ ; 1903-2012). Grey envelope is 90% confidence interval (CI) for average of annual Ba/Ca ratios. Dotted line represents 90% CI for 15yr Gaussian smoothed data. Stippled line indicates single sample extending to 1903. **b)** JJA instrumental temperature data: Sea surface temperature (SST) (ERSSTv5) for Disko Bay ( $67\text{--}71^\circ\text{N}$ ,  $55\text{--}51^\circ\text{W}$ ), Surface temperature (ST, HadCRUT5,  $65\text{--}70^\circ\text{N}$ ,  $55\text{--}45^\circ\text{W}$ ), Ilulissat station air temperature (SAT, station 4221). Black lines (annual data), green line (15pt-Gaussian filtered). Reference period (beige box) defined for 1932-2000 time period, beginning at the start of the averaged Ba/Ca master chronology. Range corresponds to  $2\sigma$  of original data before filtering. Median time of climate emergence (vertical red bars) in (a) is defined as time at which climate signal (15yr filter) first exceeds and remains above the  $+2\sigma$  threshold

185

190



(stippled horizontal line) of reference period. Change point analysis showing timing of trend change in filtered data (vertical orange bar). Orange box denotes 90% CI for change points.

195

## 2.5 Instrumental data

Modelled surface mass balance (SMB) for the GrIS is available from the Modèle Atmosphérique Régional (MAR) regional climate model (Fettweis et al., 2017). All MAR model outputs can be downloaded at <ftp://ftp.climato.be/fettweis/MARv3.5/Greenland/>. As the longer MAR 3.5.2 model data end in 2012, we additionally employ the MAR 3.1.2 (1950-2020) version for comparison to satellite and algal proxy data to include the recent decade (Fig. 3). Both versions are compared in Figure A3.

Extended Reconstructed Sea Surface Temperature Dataset, Version 5 (ERSSTv5) was used to calculate summer SST (JJA) for Disko Bay (2x2° resolution; Figures 2 and 3) averaged for 67-71°N, 55-51°W 4°x4° grid box. ERSSTs were observed by conventional thermometers in buckets (insulated or un-insulated canvas and wooden buckets), engine room intakers, or floats and drifters (Huang et al., 2017; Smith and Reynolds, 2004). Data available at <https://iridl.ledo.columbia.edu/SOURCES/.NOAA/.NCDC/.ERSST/.version5/.sst/>

High-resolution summer sea surface temperature data for JJA from NOAA Optimum Interpolation Sea Surface Temperature (OISST) v2.1 (OISSTv2p1, 1982-2020; averaged over 68.5-69.5°N, 53-51°W box; Figure 1) is based on data from NOAA NCDC: National Climatic Data Center. The NOAA 1/4° daily Optimum Interpolation Sea Surface Temperature (or daily OISST) is an analysis constructed by combining observations from different platforms (satellites, ships, buoys and Argo floats) on a regular global grid. A spatially complete SST map is produced by interpolating to fill in gaps. The methodology includes bias adjustment of satellite and ship observations (referenced to buoys) to compensate for platform differences and sensor biases. More details at <https://www.ncei.noaa.gov/products/optimum-interpolation-sst/>. Data available at [https://iridl.ledo.columbia.edu/SOURCES/.NOAA/.NCDC/.OISST/.version2p1/.AVHRR\\_monthly/.sst/](https://iridl.ledo.columbia.edu/SOURCES/.NOAA/.NCDC/.OISST/.version2p1/.AVHRR_monthly/.sst/)

Comparison of ERSSTv5 data to shorter, but higher spatial- and temporal-resolution satellite summer SST (OISSTv2p1) for Disko Bay (see Figure A4) indicates that there are significant differences in available SST data depending on the selected grid box and data resolution. OISSTv2p1 for Disko Bay shows consistently higher SSTs from around 2007 onwards (Figure 3 and Figure A4). This discrepancy in temperatures, however, can be attributed to the different temporal and spatial resolutions in SST source data, with updated high-resolution datasets showing notable differences in warming in high-Arctic regions (Huang et al., 2021). The new OISSTv2p1 product, calculated from daily satellite measurements, points to exceptional warming (>1°C/decade) taking place in western Greenland, especially in Disko Bay (Figure 1). When both SST datasets are compared for the larger grid box, observations show similar variability and annual maxima (Figure A4). By using a smaller grid box for Disko Bay (only possible with 0.25°x025° spatial resolution OISST), we can successfully resolve the stronger warming in Disko Bay, which is larger than warming in the large 4°x4° grid box that also includes part of the West Greenland coast. Due to the short time span covered by the OISSTv2p1 product it can, however, not be used to calculate emergence using the



reference period. Hence, ERSST provides useful data for assessing long-term variability and trend change. A comparison of 230 coralline algal Ba/Ca to high-resolution summer OISSTv2p1 data for the smaller Disko Bay grid box displays significant and higher correlations ( $R=0.60$ , 1982-2018, JJA; Figure 3) as compared to ERSSTv5 from the larger  $4^\circ \times 4^\circ$  grid box ( $R=0.25$ ).

HadCRUT5 is a gridded dataset of global historical surface temperature anomalies relative to a 1961-1990 reference period (Morice et al., 2021). It is available from January 1850 onwards, on a 5 degree grid and as global and regional average time series. We use it as surface temperature (ST, Figure 2) averaged for a larger box including Disko Bay ( $65\text{-}70^\circ\text{N}$ ,  $55\text{-}45^\circ\text{W}$ ).  
235 The dataset is a collaborative product of the Met Office Hadley Centre and the [Climatic Research Unit at the University of East Anglia](#). The gridded data are a blend of the [CRUTEM5](#) land-surface air temperature dataset and the [HadSST4](#) sea-surface temperature (SST) dataset. Details and data available at <https://www.metoffice.gov.uk/hadobs/hadcrut5/data/HadCRUT.5.0.2.0/download.html>.

240 Ilulissat air temperature (SAT, Figure 2) is derived from station 4221 (WMO identifier). Monthly temperature data is available for 1807-present (DMI report, DMI historical data collection; <https://www.dmi.dk/>).

245 Jakobshavn Isbrae mass loss estimation is based on historical photographs (Khan et al., 2020) (Figure 3). Data available from 1880-2012 for Jakobshavn Glacier, annual data available from 1995. Ice mass change calculated in Gigatons. Dataset available: <https://ftp.space.dtu.dk/pub/abbas/naturecomm2020/>.

250 Mass changes of the Greenland Ice Sheet observed by GRACE/GRACE-FO, relative to the long-term mean over the period 2002 through 2019 (Figure 3), are available for the entire GrIS and as basin-averaged ice-mass changes (time series of storage variations in gigatons (Gt) for 7 major drainage basins of the GrIS). Here, data for the West Greenland drainage basin is based on box 306, which includes a large part of the Jakobshavn Glacier drainage area and covers most of the central western Greenland region. Basin map and data available at <http://gravis.gfz-potsdam.de/gis> (Sasgen et al., 2020).

## 2.6 Statistical analysis

### 2.6.1 Gaussian filtering:

255 All datasets were filtered with a 15-year Gaussian kernel smoothing, available on the ‘stats’ package (v4.2. `ksmooth(3)`) for R software (R Core Team, 2023).

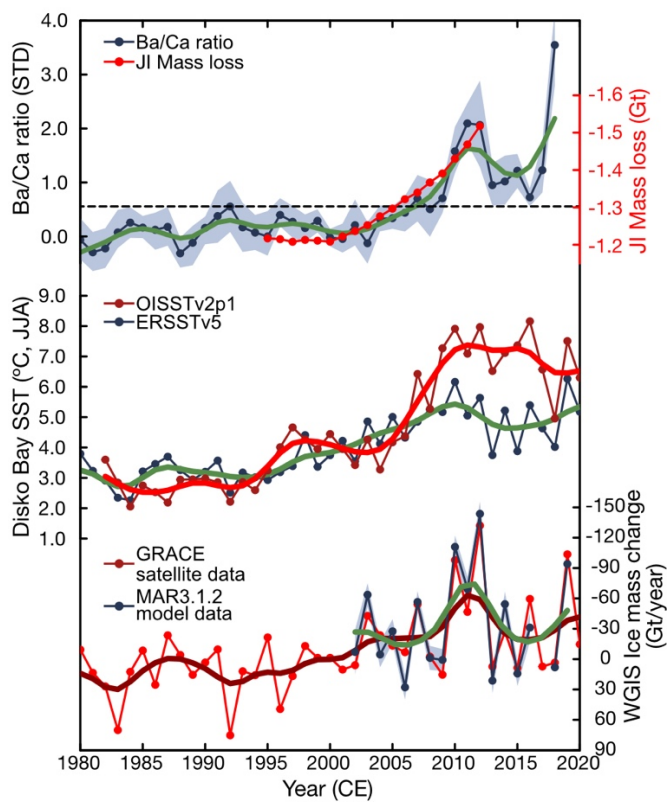
### 2.6.2 Change point analysis:

260 The smoothed Ba/Ca master chronology time series and climate data were divided into two periods using the change point analysis method (Chaudhuri and Marron, 1999). The change point analysis shows the point (i.e., year) when the trend significantly changes. The confidence interval of the change point was derived from the bootstrap technique based on the 1,000 bootstrap samples. The analysis was performed using the statistical software R (R Core Team, 2023) with SiZer (SIgnificant

ZERO crossings of derivatives) package (v. 0.1–4). The package was downloaded at <https://CRAN.R-project.org/package=SiZer>.

### 2.6.3 Time-of-emergence testing:

265 To assess whether the Ba/Ca runoff proxy and climate data have exceeded the previous range of variability and to pinpoint when this has potentially occurred we employ time-of-emergence testing. This method assesses when a climate change signal emerges above a pre-defined noise threshold (Hawkins and Sutton, 2012). We use a threshold of  $2\sigma$  of standard deviation above/below the mean of the reference period. The period from 1932 to 2000 has been selected as the reference for testing climate emergence. The starting point 1932 represents the earliest year for which at least five samples are averaged in the  
 270 Disko Bay algal master chronology. The end year (AD 2000) was selected as a time before the onset of major GrIS mass change. Median time of climate emergence (marked by vertical red bars, Fig. 2) is defined as the time at which the climate signal (15pt-Gaussian filtered) first exceeds and remains above the  $2\sigma$  threshold (stippled horizontal line) of the reference period.



275

Figure 3. Algal proxy compared to observed JI mass loss, sea surface temperature (SST) and satellite- and model-based western GrIS mass change. Recent 40 years of normalized and annually averaged algal Ba/Ca master chronology (blue; 15yr Gaussian smoothed, green) compared to Jakobshavn Isbrae (JI) mass loss calculation (Khan et al., 2020) (based on historic photographs; red). Summer SST (JJA) for Disko Bay from ERSSTv5 ( $67^{\circ}$ – $71^{\circ}$ N,  $55^{\circ}$ – $51^{\circ}$ W,  $4^{\circ}$  x  $4^{\circ}$  grid box) and OISSTv2p1 ( $0.25^{\circ}$  x  $0.25^{\circ}$  resolution; 1982–2020) for  $68.5^{\circ}$ – $69.5^{\circ}$ N,  $53^{\circ}$ – $51^{\circ}$ W box. Satellite-based mass change observations from the Gravity Recovery and Climate

280



285

**Experiment (GRACE) satellite product (western GrIS, box 306; 2002-2018,  $2\sigma$  error envelope) (Sasgen et al., 2020). MAR 3.1.2 modelled mass change for western GrIS. Comparison between algal Ba/Ca and GRACE mass change shows significant negative relationships (annual mean:  $R = -0.52$ ; for the western basin, 2002-2018). Correlations similar to ones observed for entire GrIS (annual mean:  $R = -0.61$ ; not shown). Thicker lines represent 15yr Gaussian smoothed data. Grey envelope (top) is 90% CI for average of annual Ba/Ca ratios.**

### 3 Results and Discussion

#### 3.1 Proxy relationship to glacier mass change and trends

290 Direct observations of JI runoff into Disko Bay are not available, however, changes in mass balance for recent decades and the present-day mass loss of the GrIS have been estimated from satellite-based observations (Mouginot et al., 2019; Sasgen et al., 2020; Velicogna, 2009). To extend the record further back in time we have to rely on model data. Model estimates of surface mass balance (SMB) from the Modèle Atmosphérique Régional (MAR) regional climate model (Fettweis et al., 2017) are available for the 20th century. Algal Ba/Ca ratio runoff proxy time series are compared to modelled SMB for the time 295 periods 1903-2012 (MAR3.5.2 version, Fig. 2) and 1950-2019 (MAR3.1.2 version, Figure 3). We find significant relationships between the algal Ba/Ca runoff proxy and modelled mass change and temperature data (Figure 2; Table A1). An overall trend to more negative surface mass balance is seen in model data averaged for the western GrIS starting in the late 1990s and peaking in 2012. Trend analysis has identified a change point in modelled mass change of the western GrIS (MAR3.5.2) in 1998 (Fig. 2). Satellite-based analysis of glacier terminus positions and glacier area of marine-terminating glaciers in northwest 300 and central-west Greenland (incl. JI) observed that most glaciers have retreated in the 1972-2021 time period and a step-wise acceleration in retreat rates was pinpointed to have started in most glaciers between 1996-1998 (Black and Joughin, 2022). The algal Ba/Ca master chronology matches the timing in trend acceleration in mass change (Figs. 2 and 3). We identify a trend change point in summer 2001, after which the positive trend (higher Ba/Ca corresponding to higher mass change) increases steeply, peaking in 2012 (0.101 STD/year; Fig. 2). No significant trend is detected in Ba/Ca before the change point 305 (0.01 STD/year). GrIS ice discharge observation data also show relatively steady discharge from 1986 to 2000, then increasing sharply from 2000 to 2005 (Mankoff et al., 2019), corresponding to the change point found in the algal proxy. Hence, the Ba/Ca proxy reliably detects the accelerating influence of glacial runoff into Disko Bay surface waters and mirrors an exceptional nonlinear rise in Jakobshavn Isbrae runoff. Coralline algal Ba/Ca is highly correlated to estimates of JI mass 310 loss (based on historical photographs (Khan et al., 2020);  $R=-0.91$ , 1995-2012, annual data; Fig. 3). JI mass loss data also show a steep increase in the early 2000s and a maximum in 2012, in line with the algal Ba/Ca proxy, MAR model SMB and high-resolution GRACE total mass balance satellite data (Fig. 3). In addition to trend analysis, we use "time-of-emergence-testing" to assess whether the Ba/Ca proxy and climate data have exceeded the previous range of variability and to pinpoint when this has potentially occurred. This method assesses when a climate change signal emerges above a pre-defined noise threshold (Hawkins and Sutton, 2012). Time of climate emergence 315 is detected in the algal proxy in 2007, showing that the previous range of variability of algal Ba/Ca ratios seen in the 20<sup>th</sup>



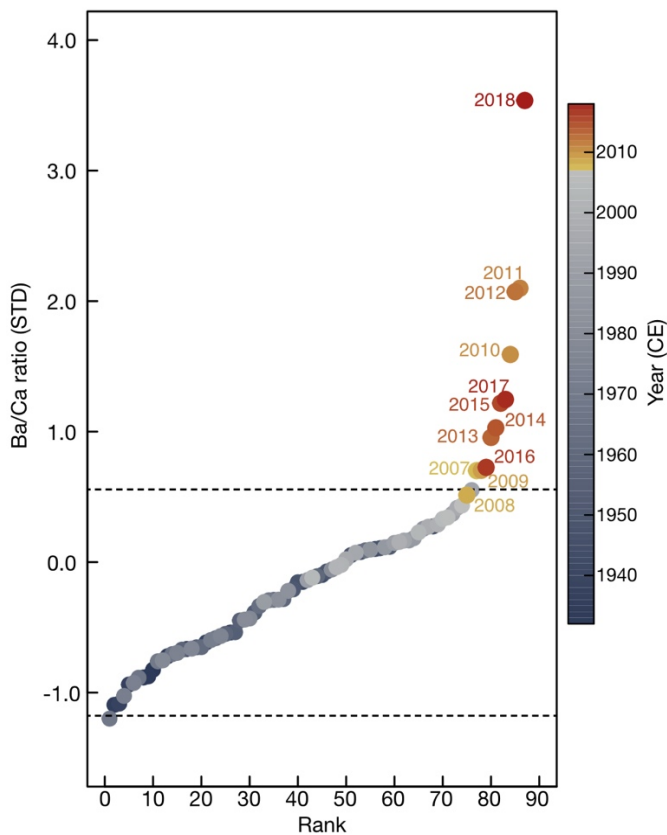
century has been exceeded for the entire remaining part of the record. This is very similar to the emergence point in modelled western GrIS SMB, which is detected in 2010 (Figure 2).

### 3.2 Relationship to temperature increase and record years

320 In south and central-west Greenland the recent retreat and speed-up of marine-terminating glaciers was mainly attributed to ocean warming (Slater and Straneo, 2022; Wood et al., 2021), with atmospheric warming also playing a significant role (Slater and Straneo, 2022). In absence of long-term direct measurement time series of subsurface ocean waters, we examine the ocean conditions that influence Disko Bay and JI by using averaged ERSSTv5 reanalysis SST data for Disko Bay (67-71°N, 55-51°W grid box). SSTs show an increasing trend from the early 1990s (SiZer analysis change point in 1993, Figure 2), rising stepwise until around 2012, then decrease slightly but remain high (Figs. 2 and 3). A similar variability and trend is observed in surface air and combined ocean and land temperature data (Fig. 2) for the region although neither dataset exhibited an emergence point, i.e. a significant excursion beyond the reference period. However, high spatial and temporal-resolution OISSTv2p1 tracks ERSSTv5 but indicates greater temperature variability and higher SSTs in the inner Disko Bay (68.5°-69.5°N, 53°-51°W grid box, 1982-2020; Figure 3, see detailed comparison between SST data and grid boxes in Methods (Huang et al., 2021) and Appendices). Updated OISSTv2p1 shows SSTs larger than 6°C after 2010 (except in 2018), suggesting that the long-term surface warming is amplified in coastal regions of western Greenland, especially in Disko Bay (Figs. 1 and 3), providing a possible explanation of accelerating glacier melt and at least to some degree runoff. However, the detected emergence in algal-based runoff variability is not yet apparent in long instrumental temperature time series (Fig. 2) and suggests a decoupling between Ba/Ca and surface temperatures. Evidence points to significant influence of variability of 335 subsurface ocean temperatures affecting the marine terminus of JI, where intrusion of warm Atlantic water masses has been linked to speed-up and disintegration of JI ice tongue in Ilulissat Icefjord (Joughin et al., 2008; Khazendar et al., 2019). Record Ba/Ca years coincide with the JI speed-up, when JI experienced maximum surface thinning (Khazendar et al., 2019). Speed-up peaked in the summer of 2012 after several years of acceleration starting in the early 2000s, matching Ba/Ca positive peaks (Fig. 3), when warmer subsurface waters entered the Ilulissat Icefjord. However, in subsurface waters the detection of "climate 340 emergence" above the threshold of natural variability is not possible due to the absence of long-term continuous observations. A drastic non-linear increase was also found in ice core-based GrIS runoff reconstructions from the central-west Greenland region (core locations situated within the JI drainage basin), which show a 250 to 575% rise in melt intensity in the first two decades of the 21<sup>st</sup> century relative to a pre-industrial baseline period (Trusel et al., 2018). When examining the entire 115-year coralline algal proxy record, earlier positive excursions in Ba/Ca comparable to the ones seen in the recent two decades 345 are absent (Figures 2 and 4). This suggests that the extreme melt years observed in satellite-based mass change estimates, and registered in algal Ba/Ca (Fig. 3), are unprecedented over the entire proxy record and on historical timescales back to at least the early 20<sup>th</sup> century. To illustrate this, we rank individual yearly Ba/Ca ratios for the entire record relative to the 1932-2000 reference period (Figure 4). All years since 2007 exceed the  $2\sigma$  threshold, clearly showing a relationship between the ascending



rank of increasing runoff and time. Hence, twelve of the highest runoff proxy years of the algal master chronology occur in  
350 the recent two decades, demonstrating the acceleration of GrIS runoff into Disko Bay.



355 **Figure 4. Ranking of record years in Ba/Ca.** Ranked annual Ba/Ca for 1903–2018 relative to 1932–2000 reference period. Year indicated by colour of filled circles. Yearly data shown before Gaussian smoothing. Labeled red and orange colored circles show years above emergence threshold (compare Fig. 2). Stippled lines define  $2\sigma$  threshold. Ba/Ca ratio years below threshold shown by grey dots (no year labels).

The sediment flux from the GrIS to the surface ocean has increased significantly, with present-day flux being already >50% higher than during the 1961–1990 period (Overeem et al., 2017). This agrees with the exceptional non-linear rise seen in our  
360 algal Ba/Ca record and suggests that the expected future acceleration of GrIS melt and ice sheet flow may further increase the delivery of sediment from Greenland to the fjord systems and the surface ocean. An increase of temperature-related surface melt, which is to be expected in the future (Noël et al., 2021; Stokes et al., 2025), has substantial influence on the sediment discharge from GrIS marine-terminating glaciers into surrounding waters (Andresen et al., 2024), also increasing particle transport from the GrIS into the oceans. In addition to having a significant regional impact, the accelerating GrIS ice loss has  
365 been listed as one of the main tipping points in the Earth's climate system (Lenton et al., 2019) due to its major influence on global ocean circulation.



Recent studies suggest that Arctic warming and GrIS melting are driving an influx of freshwater into the North Atlantic that may have contributed to a 15% slowdown of the Atlantic Meridional Overturning Circulation (AMOC), a key part of the global thermohaline circulation (Caesar et al., 2018), since the mid-20th century. The thermohaline circulation is an important  
370 regulator of the meridional heat transport in the North Atlantic and is largely responsible for the relatively warm climates of northern Europe (Kuhlbrodt et al., 2009). Increased meltwater input to the ocean from the GrIS could weaken or even disrupt the North Atlantic branch of the thermohaline circulation by increasing upper ocean stratification in the convective regions (Rahmstorf et al., 2015), although future AMOC responses will be sensitive to how the extra freshwater input is distributed  
375 (Shan et al., 2024). New modelling data suggest that the recent weakening of the AMOC can potentially be explained if meltwater from the GrIS is taken into account and that further weakening of the Atlantic overturning circulation is likely to occur much sooner than previously thought (Pontes and Menviel, 2024). Hence, rapid melting of the GrIS has wide-reaching  
380 global consequences, with a nonlinear increase in glacial runoff eventually leading to an acceleration of freshwater influx into the North Atlantic. While recent studies based on an observational campaign suggest a lesser role of the western subpolar gyre off Greenland for the origin of AMOC variability (Menary et al., 2020) as compared to the eastern subpolar gyre, it remains to be seen whether the unprecedented trend change in glacial runoff increase in Disko Bay shown here can also be identified in east Greenland marine-terminating glaciers.

## Conclusions

We present the first multi-specimen master chronology of coralline algal Ba/Ca ratios from Disko Bay, providing a seasonal-  
385 resolution reconstruction of past runoff variability. By using sample chronologies from nine long-lived coralline algal specimens, we developed a 115-year continuous proxy record. The algal-based Ba/Ca proxy reliably detects the accelerating influence of runoff into Disko Bay surface ocean waters and documents an exceptional nonlinear rise with a trend change point in summer 2001, after which the positive trend increases steeply. These results highlight the escalating impact of global warming on coastal Greenland on short time scales. Extreme GrIS melt years observed in satellite-based mass change estimates  
390 during the recent two decades are also registered in the algal Ba/Ca proxy record. By using "time-of-emergence-testing" statistics, we were able to detect that recent rates of glacial runoff recorded in algal Ba/Ca are unprecedented in the past 115 years, signalling the permanent emergence of western GrIS runoff above the 20th century reference period threshold. Our new record closes a critical observational gap by supplying the first seasonal-resolution baseline data of glacial runoff variability reaching Disko Bay surface waters, extending across the entire 20th century and into recent decades. It provides independent  
395 empirical evidence for a non-linear, accelerated response of Greenland's largest glacier, reinforcing model-based projections that a tipping point in the GrIS mass balance may be approaching. The exceptional rise in algal Ba/Ca demonstrates that contemporary meltwater and particle delivery to the coastal ocean is already substantially elevated, with likely consequences for upper-ocean stratification, regional biogeochemistry, and larger-scale impacts on global sea level and ocean circulation.



## Appendices

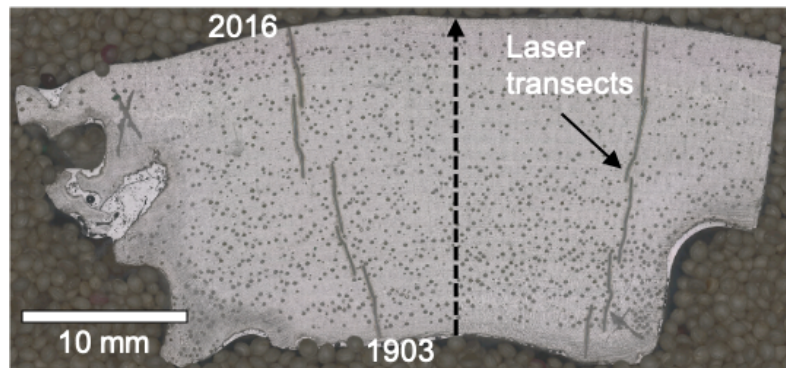


Figure A1. Polished cross-section of live-collected *Clathromorphum compactum* specimen from Disko Bay (sample 16-1-19, time period C.E. 1903-2016 covered by laser analysis). Post-analysis laser ablation sampling transects are visible. Direction of algal growth indicated by stippled black arrow.

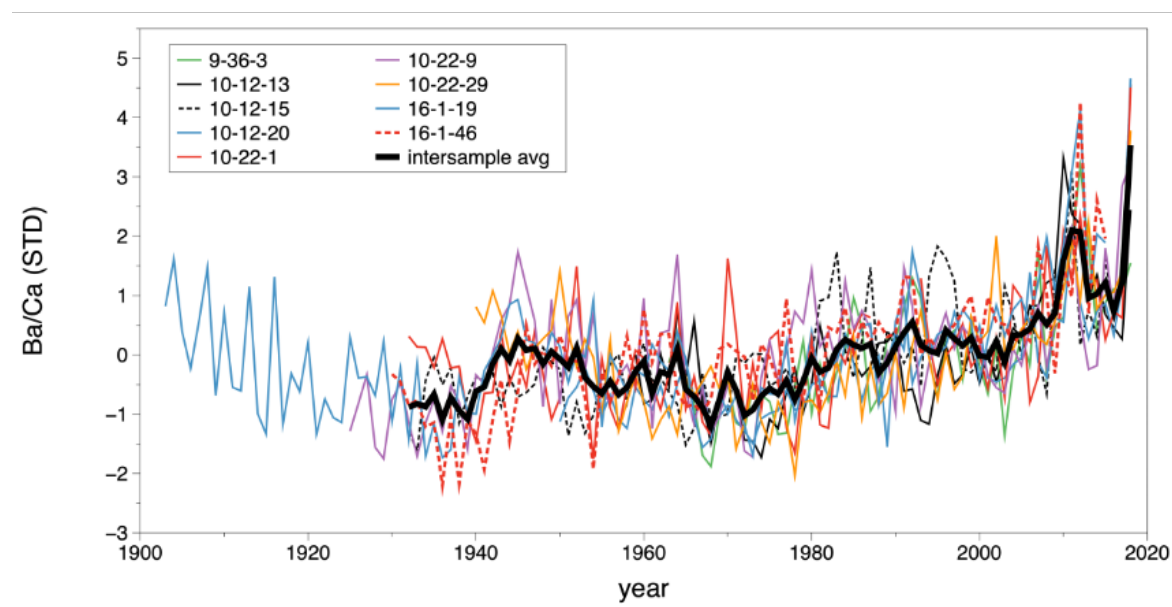
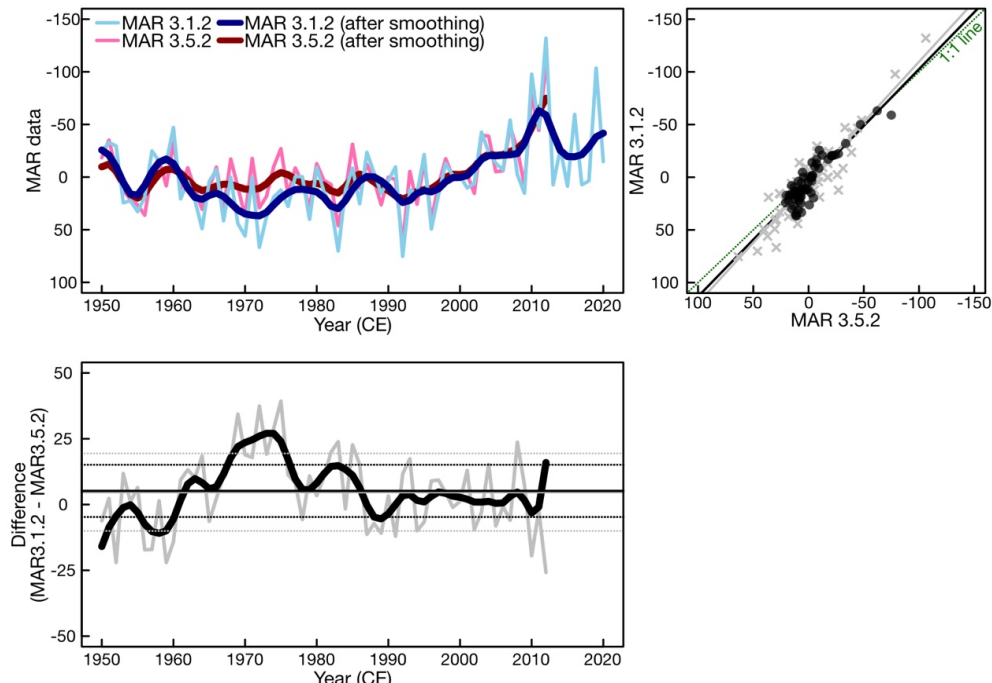


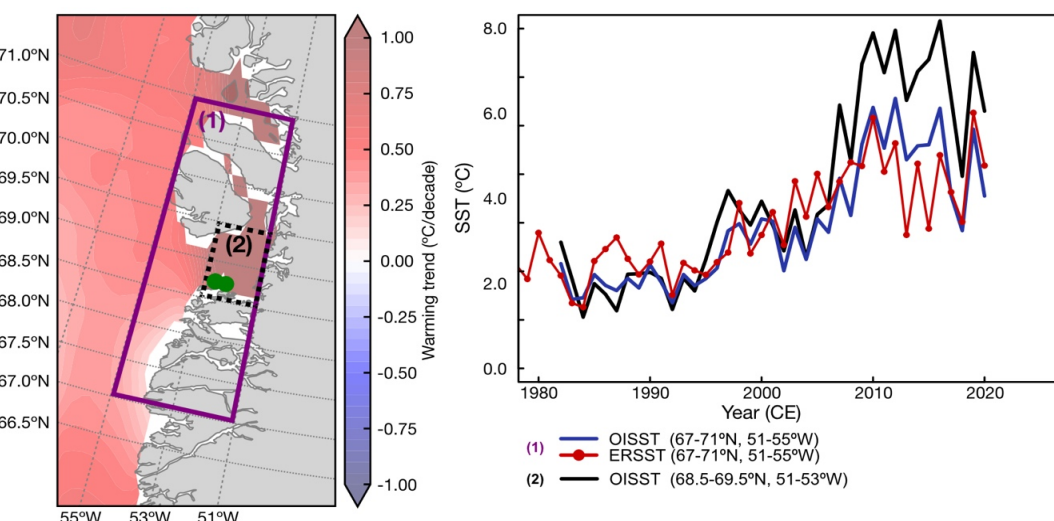
Figure A2. Ba/Ca chronologies for individual samples (two transects per sample averaged). Ba/Ca elemental ratios are shown for nine individual samples in annual resolution. Intersample average (i.e. master chronology) was calculated by averaging individual sample averages from 1932 onwards. In total the coralline algal chronologies provide 115 years of Ba/Ca ratios (C.E. 1903-2018).



415

**Figure A3.** MAR<sup>1</sup> modeled surface mass balance versions compared. Bias between versions 3.5.2 (1903-2012) and 3.1.2 (1950-2020) is minimal, especially in recent decades (e.g. from late 1980s, standard deviation is within 1 sigma level difference, dotted line). In the 1970s, MAR 3.1.2 is biased lower than 3.5.2. However, this has minimal influence on the change point detection as a similar trend is observed in both versions. In the longer record (MAR 3.1.2) the variation is magnified/higher in the earlier record (pre 1980), although correlation is still high between both versions.

420



425

**Figure A4.** Comparison of ERSST with OISST. Map (left) shows SST warming trend ( $^{\circ}\text{C}/\text{decade}$ , 1982-2020) and grid boxes for which data is presented in Figure 2 and 3. SST data (right) is shown for the large grid box of the West Greenland coast including Disko Bay ( $67^{\circ}$ - $71^{\circ}\text{N}$  and  $55^{\circ}$ - $51^{\circ}\text{W}$ ,  $4^{\circ}\times 4^{\circ}$  grid, purple box (1)) for ERSST (red line) and OISST (blue line). In addition OISST



(0.25x0.25° high-resolution satellite data, black line) is shown from the smaller Disko Bay grid box (68.5°–69.5°N and 53°–51°W, black stippled line box (2)). Green circles represent study sites.

430

Ba/Ca vs W.GIS mass change (MAR model)	Neff	R	p-value	Tau	t-value
	<b>11,20</b>	<b>-0,54</b>	<b>0,08</b>	7,22	-1,95
Ba/Ca vs ERSST	Neff	R	p-value	Tau	t-value
	<b>11,40</b>	<b>0,25</b>	<b>0,44</b>	7,62	0,81
Ba/Ca vs HadCRUT	Neff	R	p-value	Tau	t-value
	<b>7,80</b>	<b>0,62</b>	<b>0,10</b>	11,11	1,92
Ba/Ca vs SAT	Neff	R	p-value	Tau	t-value
	<b>8,00</b>	<b>0,58</b>	<b>0,13</b>	10,85	1,76

**Table A1.** Correlations calculated using 15-pt Gaussian filtered annual data using the TAU method<sup>2</sup>. The correlation is estimated as the Pearson correlation coefficient. For two time series with smoothing, we considered and adjusted the autocorrelation in them using the effective sample size (Neff). By using  $\tau$  (the time between independent values or persistence time), Neff is represented as follows:

$$\text{Neff} = n/\tau$$

$\tau$  is calculated as:

$$\tau = 1 + 2 \sum_{l=1}^{n-1} (R_{xl} \times R_{yl})$$

, where  $R_{xl}$  and  $R_{yl}$  are the autocorrelations at lag l for two-time series (X and Y). Then, Neff based on  $\tau$  value is used to estimate the student t-value.

435

440

## Data availability

All data will be made available at the PANGAEA open-access library (<https://www.pangaea.de/>) immediately after this manuscript is accepted.

445

## Author contribution

SH and JH conducted the fieldwork. JH prepared sample specimens and provided ultra-high-resolution microscopic mappings. SH and AT conducted LA-ICP-MS analyses. SH and TW analyzed the data. TW provided statistical analysis. SH wrote the



original draft of the manuscript. All coauthors provided feedback on the manuscript and have read and agreed to the submitted  
455 version of the manuscript.

### Competing interests

The authors declare that there are no competing interests.

### 460 Acknowledgements

We thank Natasha Leclerc for fieldwork assistance.

### Financial support

This research was supported by the DFG (Grant HE 6251/10-1 to S. H.). J. H. was supported by a Natural Sciences and  
465 Engineering Research Council of Canada Discovery Grant (316003).

### References

Adey, W. H., Halfar, J., and Williams, B.: Biological, physiological and ecological factors controlling high magnesium carbonate formation and producing a precision Arctic/Subarctic marine climate archive: the coralline genus *Clathromorphum* 470 Foslie emend Adey, Smithson. Contrib. Mar. Sci., 40, 1–48, <https://doi.org/DOI:10.5479/si.1943667X.40.1>, 2013.

Andresen, C. S., Karlsson, N. B., Straneo, F., Schmidt, S., Andersen, T. J., Eidam, E. F., Bjørk, A. A., Dartuemalle, N., Dyke, L. M., Vermassen, F., and Gundel, I. E.: Sediment discharge from Greenland's marine-terminating glaciers is linked with surface melt, Nat. Commun., 15, 1332, <https://doi.org/10.1038/s41467-024-45694-1>, 2024.

Ballinger, T. J., Bigalke, S., Walsh, J. E., Brettschneider, B., Thoman, R. L., Bhatt, U. S., Hanna, E., Hanssen-Bauer, I., Kim, 475 S.-J., Overland, J. E., and Wang, M.: NOAA Arctic Report Card 2023: Surface Air Temperature, <https://doi.org/10.25923/x3ta-6e63>, 2023.

Bamber, J., Broeke, M. van den, Ettema, J., Lenaerts, J., and Rignot, E.: Recent large increases in freshwater fluxes from Greenland into the North Atlantic, Geophys. Res. Lett., 39, L19501, 2012.

Bamber, J. L., Tedstone, A. J., King, M. D., Howat, I. M., Enderlin, E. M., van den Broeke, M. R., and Noel, B.: Land Ice 480 Freshwater Budget of the Arctic and North Atlantic Oceans: 1. Data, Methods, and Results, J. Geophys. Res. Oceans, 123, 1827–1837, <https://doi.org/10.1002/2017JC013605>, 2018.

Black, T. E. and Joughin, I.: Multi-decadal retreat of marine-terminating outlet glaciers in northwest and central-west Greenland, The Cryosphere, 16, 807–824, <https://doi.org/10.5194/tc-16-807-2022>, 2022.

Caesar, L., Rahmstorf, S., Robinson, A., Feulner, G., and Saba, V.: Observed fingerprint of a weakening Atlantic Ocean 485 overturning circulation, Nature, 556, 191–196, <https://doi.org/10.1038/s41586-018-0006-5>, 2018.

Chan, P., Halfar, J., Williams, B., Hetzinger, S., Steneck, R., Zack, T., and Jacob, D. E.: Freshening of the Alaska Coastal Current recorded by coralline algal Ba/Ca ratios, J. Geophys. Res., 116, G01032, 2011.



Chaudhuri, P. and Marron, J. S.: SiZer for Exploration of Structures in Curves, *J. Am. Stat. Assoc.*, 94, 807–823, <https://doi.org/10.1080/01621459.1999.10474186>, 1999.

490 Echelmeyer, K., Clarke, T. S., and Harrison, W. D.: Surficial glaciology of Jakobshavn Isbræ, West Greenland: Part I. Surface morphology, *J. Glaciol.*, 37, 368–382, <https://doi.org/10.3189/S0022143000005803>, 1991.

Evans, D., Bhatia, R., Stoll, H., and Müller, W.: LA-ICPMS Ba/Ca analyses of planktic foraminifera from the Bay of Bengal: Implications for late Pleistocene orbital control on monsoon freshwater flux, *Geochem. Geophys. Geosystems*, 16, 2598–2618, <https://doi.org/10.1002/2015GC005822>, 2015.

495 Fettweis, X., Box, J. E., Agosta, C., Amory, C., Kittel, C., Lang, C., van As, D., Machguth, H., and Gallée, H.: Reconstructions of the 1900–2015 Greenland ice sheet surface mass balance using the regional climate MAR model, *The Cryosphere*, 11, 1015–1033, <https://doi.org/10.5194/tc-11-1015-2017>, 2017.

Gillikin, D. P., Dehairs, F., Lorrain, A., Steenmans, D., Baeyens, W., and André, L.: Barium uptake into the shells of the common mussel (*Mytilus edulis*) and the potential for estuarine paleo-chemistry reconstruction, *Geochim. Cosmochim. Acta*, 500 70, 395–407, <https://doi.org/10.1016/j.gca.2005.09.015>, 2006.

Greene, C. A., Gardner, A. S., Wood, M., and Cuzzzone, J. K.: Ubiquitous acceleration in Greenland Ice Sheet calving from 1985 to 2022, *Nature*, 625, 523–528, <https://doi.org/10.1038/s41586-023-06863-2>, 2024.

Grove, C. A., Zinke, J., Peeters, F., Park, W., Scheufen, T., Kasper, S., Randriamanantsoa, B., McCulloch, M. T., and Brummer, G.-J. A.: Madagascar corals reveal a multidecadal signature of rainfall and river runoff since 1708, *Clim Past*, 9, 505 641–656, <https://doi.org/10.5194/cp-9-641-2013>, 2013.

Guay, C. K. and Kenison Falkner, K.: A survey of dissolved barium in the estuaries of major Arctic rivers and adjacent seas, *Cont. Shelf Res.*, 18, 859–882, [https://doi.org/10.1016/S0278-4343\(98\)00023-5](https://doi.org/10.1016/S0278-4343(98)00023-5), 1998.

Guo, Y., Al-Hashem, A. A., Krisch, S., Hopwood, M. J., Chen, X.-G., and Achterberg, E. P.: Distributions, sources, and dynamics of particulate Ba, Cr, Sr, Zn, Mo, W, Th, and U on the Northeast Greenland Shelf, *Chem. Geol.*, 686, 122822, 510 <https://doi.org/10.1016/j.chemgeo.2025.122822>, 2025.

Halfar, J., Adey, W. H., Kronz, A., Hetzinger, S., Edinger, E., and Fitzhugh, W. W.: Arctic sea-ice decline archived by multicentury annual-resolution record from crustose coralline algal proxy, *Proc. Natl. Acad. Sci.*, 110, 19737–19741, <https://doi.org/10.1073/pnas.1313775110>, 2013.

Hanna, E., Cappelen, J., Fettweis, X., Mernild, S. H., Mote, T. L., Mottram, R., Steffen, K., Ballinger, T. J., and Hall, R. J.: 515 Greenland surface air temperature changes from 1981 to 2019 and implications for ice-sheet melt and mass-balance change, *Int. J. Climatol.*, 41, E1336–E1352, <https://doi.org/10.1002/joc.6771>, 2021.

Hansen, M. O., Nielsen, T. G., Stedmon, C. A., and Munk, P.: Oceanographic regime shift during 1997 in Disko Bay, Western Greenland, *Limnol. Oceanogr.*, 57, 634–644, <https://doi.org/10.4319/lo.2012.57.2.0634>, 2012.

Hawkins, J. R., Skidmore, M. L., Wadham, J. L., Priscu, J. C., Morton, P. L., Hatton, J. E., Gardner, C. B., Kohler, T. J., 520 Stibal, M., Bagshaw, E. A., Steigmeyer, A., Barker, J., Dore, J. E., Lyons, W. B., Tranter, M., Spencer, R. G. M., and the



SALSA Science Team: Enhanced trace element mobilization by Earth's ice sheets, *Proc. Natl. Acad. Sci.*, 117, 31648–31659, <https://doi.org/10.1073/pnas.2014378117>, 2020.

Hawkins, E. and Sutton, R.: Time of emergence of climate signals, *Geophys. Res. Lett.*, 39, <https://doi.org/10.1029/2011GL050087>, 2012.

525 Hetzinger, S., Halfar, J., Zack, T., Gamboa, G., Jacob, D. E., Kunz, B. E., Kronz, A., Adey, W., Lebednik, P. A., and Steneck, R. S.: High-resolution analysis of trace elements in crustose coralline algae from the North Atlantic and North Pacific by laser ablation ICP-MS, *Palaeogeogr. Palaeoclimatol. Palaeoecol.*, 302, 81–94, 2011.

Hetzinger, S., Halfar, J., Zajacz, Z., and Wissak, M.: Early start of 20th-century Arctic sea-ice decline recorded in Svalbard coralline algae, *Geology*, 47, 963–967, <https://doi.org/10.1130/G46507.1>, 2019.

530 Hetzinger, S., Halfar, J., Zajacz, Z., Möller, M., and Wissak, M.: Late twentieth century increase in northern Spitsbergen (Svalbard) glacier-derived runoff tracked by coralline algal Ba/Ca ratios, *Clim. Dyn.*, 56, 3295–3303, <https://doi.org/10.1007/s00382-021-05642-x>, 2021.

Hofer, S., Tedstone, A. J., Fettweis, X., and Bamber, J. L.: Decreasing cloud cover drives the recent mass loss on the Greenland Ice Sheet, *Sci. Adv.*, 3, <https://doi.org/10.1126/sciadv.1700584>, 2017.

535 Holland, D. M., Thomas, R. H., de Young, B., Ribergaard, M. H., and Lyberth, B.: Acceleration of Jakobshavn Isbrae triggered by warm subsurface ocean waters, *Nat. Geosci.*, 1, 659–664, [http://www.nature.com/ngeo/journal/v1/n10/supplinfo/ngeo316\\_S1.html](http://www.nature.com/ngeo/journal/v1/n10/supplinfo/ngeo316_S1.html), 2008.

Hopwood, M. J., Carroll, D., Gu, Y., Huang, X., Krause, J., Cozzi, S., Cantoni, C., Gastelu Barcena, M. F., Carroll, S., and Körtzinger, A.: A Close Look at Dissolved Silica Dynamics in Disko Bay, West Greenland, *Glob. Biogeochem. Cycles*, 39,

540 e2023GB008080, <https://doi.org/10.1029/2023GB008080>, 2025.

Hörhold, M., Münch, T., Weißbach, S., Kipfstuhl, S., Freitag, J., Sasgen, I., Lohmann, G., Vinther, B., and Laepple, T.: Modern temperatures in central–north Greenland warmest in past millennium, *Nature*, 613, 503–507, <https://doi.org/10.1038/s41586-022-05517-z>, 2023.

545 Huang, B., Thorne, P. W., Banzon, V. F., Boyer, T., Chepurin, G., Lawrimore, J. H., Menne, M. J., Smith, T. M., Vose, R. S., and Zhang, H.-M.: Extended Reconstructed Sea Surface Temperature, Version 5 (ERSSTv5): Upgrades, Validations, and Intercomparisons, *J. Clim.*, 30, 8179–8205, <https://doi.org/10.1175/JCLI-D-16-0836.1>, 2017.

Huang, B., Liu, C., Banzon, V., Freeman, E., Graham, G., Hankins, B., Smith, T., and Zhang, H.-M.: Improvements of the Daily Optimum Interpolation Sea Surface Temperature (DOISST) Version 2.1, *J. Clim.*, 34, 2923–2939, <https://doi.org/10.1175/JCLI-D-20-0166.1>, 2021.

550 Joughin, I., Abdalati, W., and Fahnestock, M.: Large fluctuations in speed on Greenland's Jakobshavn Isbræ glacier, *Nature*, 432, 608, <https://doi.org/10.1038/nature03130>, 2004.

Joughin, I., Das, S. B., King, M. A., Smith, B. E., Howat, I. M., and Moon, T.: Seasonal Speedup Along the Western Flank of the Greenland Ice Sheet, *SCience*, 320, 781–783, <https://doi.org/10.1126/science.1153288>, 2008.



555 Joughin, I., Alley, R. B., and Holland, D. M.: Ice-Sheet Response to Oceanic Forcing, SCience, 338, 1172–1176,  
https://doi.org/10.1126/science.1226481, 2012.

Joughin, I., Shean, D. E., Smith, B. E., and Floricioiu, D.: A decade of variability on Jakobshavn Isbræ: ocean temperatures  
pace speed through influence on mélange rigidity, The Cryosphere, 14, 211–227, <https://doi.org/10.5194/tc-14-211-2020>,  
2020.

560 Karlsson, N. B., Mankoff, K. D., Solgaard, A. M., Larsen, S. H., How, P. R., Fausto, R. S., and Sørensen, L. S.: A data set of  
monthly freshwater fluxes from the Greenland ice sheet's marine-terminating glaciers on a glacier–basin scale 2010–2020,  
GEUS Bull., 53, <https://doi.org/10.34194/geusb.v53.8338>, 2023.

565 Khan, S. A., Bjørk, A. A., Bamber, J. L., Morlighem, M., Bevis, M., Kjær, K. H., Mouginot, J., Løkkegaard, A., Holland, D.  
M., Aschwanden, A., Zhang, B., Helm, V., Korsgaard, N. J., Colgan, W., Larsen, N. K., Liu, L., Hansen, K., Barletta, V.,  
Dahl-Jensen, T. S., Søndergaard, A. S., Csatho, B. M., Sasgen, I., Box, J., and Schenk, T.: Centennial response of Greenland's  
three largest outlet glaciers, Nat. Commun., 11, 5718, <https://doi.org/10.1038/s41467-020-19580-5>, 2020.

Khazendar, A., Fenty, I. G., Carroll, D., Gardner, A., Lee, C. M., Fukumori, I., Wang, O., Zhang, H., Seroussi, H., Moller, D.,  
Noël, B. P. Y., van den Broeke, M. R., Dinardo, S., and Willis, J.: Interruption of two decades of Jakobshavn Isbrae acceleration  
and thinning as regional ocean cools, Nat. Geosci., 12, 277–283, <https://doi.org/10.1038/s41561-019-0329-3>, 2019.

570 King, M. D., Howat, I. M., Jeong, S., Noh, M. J., Wouters, B., Noël, B., and van den Broeke, M. R.: Seasonal to decadal  
variability in ice discharge from the Greenland Ice Sheet, The Cryosphere, 12, 3813–3825, <https://doi.org/10.5194/tc-12-3813-2018>, 2018.

King, M. D., Howat, I. M., Candela, S. G., Noh, M. J., Jeong, S., Noël, B. P. Y., van den Broeke, M. R., Wouters, B., and  
Negrete, A.: Dynamic ice loss from the Greenland Ice Sheet driven by sustained glacier retreat, Commun. Earth Environ., 1,  
1, <https://doi.org/10.1038/s43247-020-0001-2>, 2020.

575 Kniest, J. F., Evans, D., Gerdes, A., Cantine, M., Todd, J. A., Sigwart, J. D., Vellekoop, J., Müller, W., Voigt, S., and Raddatz,  
J.: Spatiotemporal changes in riverine input into the Eocene North Sea revealed by strontium isotope and barium analysis of  
bivalve shells, Sci. Rep., 14, 28806, <https://doi.org/10.1038/s41598-024-79779-0>, 2024.

Krause, J., Hopwood, M. J., Höfer, J., Krisch, S., Achterberg, E. P., Alarcón, E., Carroll, D., González, H. E., Juul-Pedersen,  
T., Liu, T., Lodeiro, P., Meire, L., and Rosing, M. T.: Trace Element (Fe, Co, Ni and Cu) Dynamics Across the Salinity  
580 Gradient in Arctic and Antarctic Glacier Fjords, Front. Earth Sci., 9, 2021.

Kuhlbrodt, T., Rahmstorf, S., Zickfeld, K., Vikebo, F. B., Sundby, S., Hofmann, M., Link, P. M., Bondeau, A., Cramer, W.,  
and Jaeger, C.: An Integrated Assessment of changes in the thermohaline circulation, Clim. Change, 96, 489–537, 2009.

Latuta, L., Smedsrød, L. H., Darelius, E., Hansen, P. J., and Willis, J. K.: Drivers of seasonal hydrography in Disko Bay,  
Greenland, EGUsphere, 2025, 1–28, <https://doi.org/10.5194/egusphere-2025-1492>, 2025.

585 Lenton, T. M., Rockström, J., Gaffney, O., Rahmstorf, S., Richardson, K., Steffen, W., and Schellnhuber, H. J.: Climate tipping  
points — too risky to bet against, Nature, 575, 592–595, 2019.



Mankoff, K. D., Colgan, W., Solgaard, A., Karlsson, N. B., Ahlstrøm, A. P., van As, D., Box, J. E., Khan, S. A., Kjeldsen, K. K., Mouginot, J., and Fausto, R. S.: Greenland Ice Sheet solid ice discharge from 1986 through 2017, *Earth Syst Sci Data*, 11, 769–786, <https://doi.org/10.5194/essd-11-769-2019>, 2019.

590 Martin, T. and Biastoch, A.: On the ocean's response to enhanced Greenland runoff in model experiments: relevance of mesoscale dynamics and atmospheric coupling, *Ocean Sci.*, 19, 141–167, <https://doi.org/10.5194/os-19-141-2023>, 2023.

Mascarenhas, V. J. and Zielinski, O.: Hydrography-Driven Optical Domains in the Vaigat-Disko Bay and Godthabsfjord: Effects of Glacial Meltwater Discharge, *Front. Mar. Sci.*, 6, <https://doi.org/10.3389/fmars.2019.00335>, 2019.

McCulloch, M. T., Fallon, S., Wyndham, T., Hendy, E., Lough, J. M., and Barnes, D. J.: Coral record of increased sediment flux to the inner Great Barrier Reef since European settlement, *Nature*, 421, 727–730, 2003.

595 Menary, M. B., Jackson, L. C., and Lozier, M. S.: Reconciling the Relationship Between the AMOC and Labrador Sea in OSNAP Observations and Climate Models, *Geophys. Res. Lett.*, 47, e2020GL089793, <https://doi.org/10.1029/2020GL089793>, 2020.

Morice, C. P., Kennedy, J. J., Rayner, N. A., Winn, J. P., Hogan, E., Killick, R. E., Dunn, R. J. H., Osborn, T. J., Jones, P. D., 600 and Simpson, I. R.: An Updated Assessment of Near-Surface Temperature Change From 1850: The HadCRUT5 Data Set, *J. Geophys. Res. Atmospheres*, 126, e2019JD032361, <https://doi.org/10.1029/2019JD032361>, 2021.

Mouginot, J., Rignot, E., Bjørk, A. A., van den Broeke, M., Millan, R., Morlighem, M., Noël, B., Scheuchl, B., and Wood, M.: Forty-six years of Greenland Ice Sheet mass balance from 1972 to 2018, *Proc. Natl. Acad. Sci.*, 201904242, <https://doi.org/10.1073/pnas.1904242116>, 2019.

605 Nick, F. M., Vieli, A., Andersen, M. L., Joughin, I., Payne, A., Edwards, T. L., Pattyn, F., and van de Wal, R. S. W.: Future sea-level rise from Greenland's main outlet glaciers in a warming climate, *Nature*, 497, 235–238, <https://doi.org/10.1038/nature12068%2520http://www.nature.com/nature/journal/v497/n7448/abs/nature12068.html%2523supplementary-information>, 2013.

Noël, B., van Kampenhout, L., Lenaerts, J. T. M., van de Berg, W. J., and van den Broeke, M. R.: A 21st Century Warming 610 Threshold for Sustained Greenland Ice Sheet Mass Loss, *Geophys. Res. Lett.*, 48, e2020GL090471, <https://doi.org/10.1029/2020GL090471>, 2021.

Otosaka, I. N., Shepherd, A., Ivins, E. R., Schlegel, N. J., Amory, C., van den Broeke, M. R., Horwath, M., Joughin, I., King, M. D., Krinner, G., Nowicki, S., Payne, A. J., Rignot, E., Scambos, T., Simon, K. M., Smith, B. E., Sørensen, L. S., Velicogna, I., Whitehouse, P. L., A, G., Agosta, C., Ahlstrøm, A. P., Blazquez, A., Colgan, W., Engdahl, M. E., Fettweis, X., Forsberg, 615 R., Gallée, H., Gardner, A., Gilbert, L., Gourmelen, N., Groh, A., Gunter, B. C., Harig, C., Helm, V., Khan, S. A., Kittel, C., Konrad, H., Langen, P. L., Lecavalier, B. S., Liang, C. C., Loomis, B. D., McMillan, M., Melini, D., Mernild, S. H., Mottram, R., Mouginot, J., Nilsson, J., Noël, B., Pattle, M. E., Peltier, W. R., Pie, N., Roca, M., Sasgen, I., Save, H. V., Seo, K. W., Scheuchl, B., Schrama, E. J. O., Schröder, L., Simonsen, S. B., Slater, T., Spada, G., Sutterley, T. C., Vishwakarma, B. D., van Wessem, J. M., Wiese, D., van der Wal, W., and Wouters, B.: Mass balance of the Greenland and Antarctic ice sheets 620 from 1992 to 2020, *Earth Syst Sci Data*, 15, 1597–1616, <https://doi.org/10.5194/essd-15-1597-2023>, 2023.



Overeem, I., Hudson, B. D., Syvitski, J. P. M., Mikkelsen, A. B., Hasholt, B., van den Broeke, M. R., Noël, B. P. Y., and Morlighem, M.: Substantial export of suspended sediment to the global oceans from glacial erosion in Greenland, *Nat. Geosci.*, 10, 859–863, <https://doi.org/10.1038/ngeo3046>, 2017.

Paillard, D., Labeyrie, L., and Yiou, P.: Macintosh program performs time-series analysis, *Eos Trans. AGU*, 77, 379, 1996.

625 Pontes, G. M. and Menviel, L.: Weakening of the Atlantic Meridional Overturning Circulation driven by subarctic freshening since the mid-twentieth century, *Nat. Geosci.*, <https://doi.org/10.1038/s41561-024-01568-1>, 2024.

R Core Team: R: A Language and Environment for Statistical Computing, 2023.

Rahmstorf, S., Box, J. E., Feulner, G., Mann, M. E., Robinson, A., Rutherford, S., and Schaffernicht, E. J.: Exceptional twentieth-century slowdown in Atlantic Ocean overturning circulation, *Nat. Clim. Change*, 630 <https://doi.org/10.1038/nclimate2554>, 2015.

Rignot, E., Koppes, M., and Velicogna, I.: Rapid submarine melting of the calving faces of West Greenland glaciers, *Nat. Geosci.*, 3, 187–191, 2010.

635 Sasgen, I., Wouters, B., Gardner, A. S., King, M. D., Tedesco, M., Landerer, F. W., Dahle, C., Save, H., and Fettweis, X.: Return to rapid ice loss in Greenland and record loss in 2019 detected by the GRACE-FO satellites, *Commun. Earth Environ.*, 1, 8, <https://doi.org/10.1038/s43247-020-0010-1>, 2020.

Shan, X., Sun, S., Wu, L., and Spall, M.: Role of the Labrador Current in the Atlantic Meridional Overturning Circulation response to greenhouse warming, *Nat. Commun.*, 15, 7361, <https://doi.org/10.1038/s41467-024-51449-9>, 2024.

Slater, D. A. and Straneo, F.: Submarine melting of glaciers in Greenland amplified by atmospheric warming, *Nat. Geosci.*, 15, 794–799, <https://doi.org/10.1038/s41561-022-01035-9>, 2022.

640 Smith, T. M. and Reynolds, R. W.: Improved extended reconstruction of SST (1854–1997), *J. Clim.*, 17, 2466–2477, 2004.

Stokes, C. R., Bamber, J. L., Dutton, A., and DeConto, R. M.: Warming of +1.5 °C is too high for polar ice sheets, *Commun. Earth Environ.*, 6, 351, <https://doi.org/10.1038/s43247-025-02299-w>, 2025.

Tedesco, M. and Fettweis, X.: Unprecedented atmospheric conditions (1948–2019) drive the 2019 exceptional melting season over the Greenland ice sheet, *The Cryosphere*, 14, 1209–1223, <https://doi.org/10.5194/tc-14-1209-2020>, 2020.

645 Trusel, L. D., Das, S. B., Osman, M. B., Evans, M. J., Smith, B. E., Fettweis, X., McConnell, J. R., Noël, B. P. Y., and van den Broeke, M. R.: Nonlinear rise in Greenland runoff in response to post-industrial Arctic warming, *Nature*, 564, 104–108, <https://doi.org/10.1038/s41586-018-0752-4>, 2018.

Velicogna, I.: Increasing rates of ice mass loss from the Greenland and Antarctic ice sheets revealed by GRACE, *Geophys Res Lett*, 36, L19503, <https://doi.org/10.1029/2009gl040222>, 2009.

650 Weldeab, S., Lea, D. W., Schneider, R. R., and Anderson, N.: 155,000 years of West African monsoon and ocean thermal evolution, *SCience*, 316, 1303–1307, 2007.

Wood, M., Rignot, E., Fenty, I., An, L., Bjørk, A., van den Broeke, M., Cai, C., Kane, E., Menemenlis, D., Millan, R., Morlighem, M., Mouginot, J., Noël, B., Scheuchl, B., Velicogna, I., Willis, J. K., and Zhang, H.: Ocean forcing drives glacier retreat in Greenland, *Sci. Adv.*, 7, eaba7282, <https://doi.org/10.1126/sciadv.aba7282>, 2021.



655 Yamazaki, A., Yano, M., Harii, S., and Watanabe, T.: Effects of light on the Ba/Ca ratios in coral skeletons, *Chem. Geol.*, 559, 119911, <https://doi.org/10.1016/j.chemgeo.2020.119911>, 2021.